# A Probabilistic Approach for Vision-Based Fire Detection in Videos

Paulo Vinicius Koerich Borges, *Member, IEEE,* and Ebroul Izquierdo, *Senior Member, IEEE*

***Abstract*—Automated fire detection is an active research topic in computer vision. In this paper, we propose and analyze a new method for identifying fire in videos. Computer vision-based fire detection algorithms are usually applied in closed-circuit television surveillance scenarios with controlled background. In contrast, the proposed method can be applied not only to surveillance but also to automatic video classification for retrieval of fire catastrophes in databases of newscast content. In the latter case, there are large variations in fire and background characteristics depending on the video instance. The proposed method analyzes the frame-to-frame changes of specific low-level features describing potential fire regions. These features are color, area size, surface coarseness, boundary roughness, and skewness within estimated fire regions. Because of flickering and random characteristics of fire, these features are powerful discriminants. The behavioral change of each one of these features is evaluated, and the results are then combined according to the Bayes classifier for robust fire recognition. In addition, *a priori* knowledge of fire events captured in videos is used to significantly improve the classification results. For edited newscast videos, the fire region is usually located in the center of the frames. This fact is used to model the probability of occurrence of fire as a function of the position. Experiments illustrated the applicability of the method.**

***Index Terms*—Fire detection, probabilistic pattern recognition, video processing.**

## I. Introduction

AUTOMATED retrieval of events in newscast videos has received great attention by the research community in the last decade [1], [2]. This has been mainly motivated by the interest of broadcasters in building large digital archives of structured assets ready for search, retrieval, and reuse. A significant amount of time and money is spent by news networks to find in their archives events related to newly occurred event. In this context, catastrophe-related news are one of the most common topics that require automated retrieval, which require faster than real-time analysis. As a consequence, this task has recently been subject to large research projects such as [3] and [4]. In the catastrophe news scope, fire events are one of the most common topics, along with bombings and floods [5]. Therefore, efficient detection of fire in video contents has proved to be an important research topic in the last few years [3], [6], and [7]. Beyond classification of video content for search and retrieval, fire detection usually finds application in surveillance and related security systems.

In this paper, we propose an efficient vision-based event detection method for identifying fire in videos, extending the work presented in [8]. Most vision-based fire detection techniques proposed in the literature target surveillance applications with static cameras and consequently reasonably controlled or static background. Otherwise, they propose the use of filter banks [9], frequency transforms [10], and motion tracking, requiring more computational processing time, making them unsuitable for video retrieval.

In contrast, the proposed method is very efficient and robust when applied to detect fire catastrophes in news content. The proposed method analyses the frame-to-frame changes of specific low-level features describing potential fire regions. Five features, namely color, area size, region coarseness, boundary roughness and skewness within estimated fire regions, are used as low-level descriptors for the proposed analysis. Because of flickering and random characteristics of fire due the combustion and air flow, these are efficient classifying features. The change of each of these features is evaluated, and the results are combined according to the Bayes classifier to determine whether or not fire occurs in that frame.

In contrast to some works from the literature [11], the goal of this paper is not to identify fire pixels in a given image or video frame, but to determine if fire occurs in the frame. The goal is generic event detection for automatic classification, annotation and retrieval.

The majority of the vision-based fire detection systems employ some type of hybrid model combining color, geometry and motion information. In general, fire detection systems use color clues as a precondition to generate seed areas for possible fire regions [called a "potential fire mask" (PFM) in this paper] since color is the most discerning feature. An effective color model for potential fire pixel determination is thus essential for almost any vision-based fire detection system. Under these circumstances, the contributions presented in this paper can be listed as follows.

Manuscript received April 1, 2009; revised September 9, 2009. First version published March 15, 2010; current version published May 5, 2010. This work was supported by the European Commission (Information Society Technologies Multimedia Semantic Syndication for Enhanced News Services 6th Framework Programme) and the Australian Commonwealth Scientific and Industrial Research Organisation Information and Communication Technologies Center. This paper was recommended by Associate Editor C. N. Taylor.

P. Borges is with the Autonomous System Laboratory, Information and Communication Technologies Center, Australian Commonwealth Scientific and Industrial Research Organization (CSIRO), Pullenvale, QLD 4069, Australia (e-mail: paulo.borges@csiro.au; vini@ieee.org).

E. Izquierdo is with the Multimedia and Vision Research Group, Department of Electronic Engineering and Computer Science, Queen Mary, University of London, London E1 4NS, U.K. (e-mail: ebroul.izquierdo@elec.qmul.ac.uk).

Color versions of one or more of the figures in this paper are available online at http://ieeexplore.ieee.org.

Digital Object Identifier 10.1109/TCSVT.2010.2045813

1) A probabilistic model for color-based fire detection is proposed, which outputs a degree of confidence for each pixel as representing fire or not. We illustrate that an efficient PFM can be generated from this model. This approach can be directly employed to different fire detection methods proposed in the literature (discussed in Section II) that used color to indicate candidate fire regions.
2) Unlike many works in the literature which use shape descriptors to analyze the amount of flame motion, we use the boundary roughness of the potential fire regions. This brings the same amount of discernibility with a more efficient processing speed.
3) It has been frequently observed in the literature [12] that saturation occurs in the red channel of fire regions. In order to exploit this characteristic, we use of the third order statistical moment (skewness) of the potential fire region as a feature. This is a simple and powerful discriminant, which significantly enhances the detection performance.
4) We also propose the use of the variance as a feature, due to the randomness/coarseness observed in fire surfaces.
5) For real fire regions, the amount of fire varies from frame to frame due to flame flickering. Therefore, the change in fire area is also used as a feature with classification power.
6) For edited newscast videos, the fire region is usually located in the center of the frames. This fact is used to model the probability of occurrence of fire as a function of the position, enhancing the performance of the algorithm.
7) The features are combined with the Bayes classifier to achieve an practical low detection error rate.

This paper is organized as follows. In Section II we review existing techniques, comparing them with the proposed method. In Section III, we discuss color, semantic and dynamic fire characteristics, proposing efficient discrimination features for fire. In Section IV we propose a framework for classification, based on the Bayes classifier. In Section V we present experimental results, followed by a relevant conclusion in Section VI.

## II. Related Methods

Despite a growing interest in the topic, there is still not a large number of papers about fire detection in the computer vision literature. Many fire detection systems are based on satellite images or thermal analysis of satellite sensors [13]–[15]. However, this type of application is out of the scope of this paper. Inside the vision-based scope, the first works used purely a color-based model [16], which is the initial step for many other algorithms, including the one proposed in this paper.

An earlier version of the work presented in this paper is given in [8]. A key difference between both approaches is the use of the probabilistic approach in the color analysis, as in [8] a naive threshold is used. Apart from that, in [8] the authors do not exploit the spatial distribution of fire (discussed in Section III-F) nor present a error rate analysis for the method.

In [17], the authors use pixel colors and their temporal variations. They use an approach that is based upon creating a Gaussian-smoothed color histogram to determine the fire-colored pixels, and then using the temporal variation of pixels to determine which of these pixels are actually fire. However, this algorithm is also essentially color based, and does not exploit other statistical characteristics of potential fire regions. In addition, temporal variation in image pixel color does not capture the temporal property of fire which is more complex and benefits from a region level representation. As observed in [10], for example, pixels in the core of the fire exhibit less temporal variation than the other pixels.

An alternative approach in color-based detection is to analyze the *YCvCr* color space instead of the *RGB* space [11], [18]. In [11], for example, the authors propose the use of a fuzzy logic approach which uses luminance and chrominance information to replace the existing heuristic rules used to generate the PFM. The implicit uncertainties in the rules obtained from repeated experiments can be encoded in a fuzzy representation that is expressed in linguistic terms. The authors argue that the single output decision quantity will then give a better likelihood that a pixel is a fire pixel. Although a very good detection rate is achieved, the method is focused on images and random changes of fire from frame to frame are not exploited.

The works presented by Toreyin *et al*. in [9] and [19] also yield good results, where boundary of flames are represented in wavelet domain and high frequency nature of the boundaries of fire regions is also used as a clue to model the flame flicker spatially. However, the approach used presents two drawbacks: first, the algorithm assumes that the camera is stationary; and second, it presents a high computational complexity despite working in real-time. Considering that newscast videos have at least 25 frames/s, the analysis would be very time consuming for video retrieval applications. A similar situation occurs in the work presented in [10], which makes use of the Fourier transform for boundary description of every potential fire region.

A more recent approach presented in [20] combines spectral, spatial and temporal characteristics of fire and smoke using fuzzy logic to indicated potential candidate fire regions. The fuzzy logic reasoning, in this case, is the counterpart of our probabilistic approach proposed in Section III. Fuzzy logic is also used in [21] to fuse features like average intensity, average hue and average flickering. In both [20] and [21], however, the assumptions and reported experiments consider a static camera, which is often not the case in newscast videos.

In [22], the authors also use a probabilist metric to threshold potential fire pixels. This is achieved by multiplying the probabilities of each individual color channel being fire. However, this metric can be very sensitive: if the value of one of the channels is not very close to the expected stochastic mean for that channel, the result of the metric is significantly decreased, increasing the number of false-negatives. The probabilistic

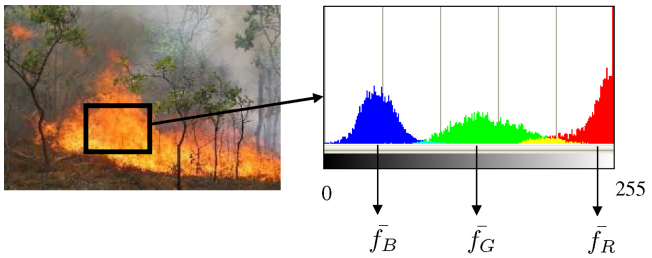


Fig. 1. Histogram of a fire region inside the black square, for the red, green, and blue channels.

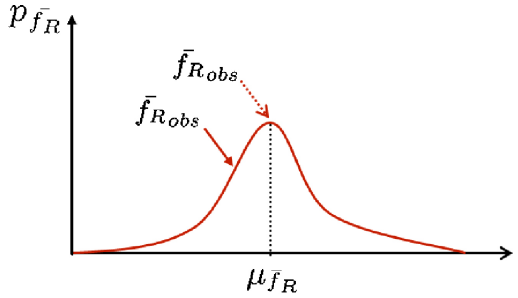


Fig. 2. Graphical representation of the parameters in (1). Maximum confidence is obtained when $\bar{f}_{R\text{obs}} = \mu_{\bar{f}_R}$.

metric for thresholding potential fire pixels that we propose in this paper minimizes this effect.

## III. Statistical Characteristics of Fire

It is well known that fire has unique visual signatures. Color, geometry, and motion of fire region are all essential features for efficient classification. In general, in addition to color, a region that corresponds to fire can be captured in terms of the spatial structure defined by the boundary variation within the region. The shape of a fire region often keeps changing and exhibits a stochastic motion, which depends on surrounding environmental factors such as the type of burning elements and wind.

Based on these factors, in the following we propose several useful features for detecting fire: color (Section III-A), randomness of fire area size (Section III-B), fire boundary roughness (Section III-C), surface coarseness (Section III-D), skewness (Section III-E), and spatial distribution (Section III-F). We explain the physical characteristics that validate their applicability.

### A. Color

According to most fire detection papers presented in the literature and based on our own experiments, we notice that fire has very distinct color characteristics, and although empirical, it is the most powerful single feature for finding fire in video sequences. Based on tests with several images in different resolutions and scenarios, it is reasonable to assume that generally the color of flames belongs to the red-yellow range. Laboratory experiments show that this is indeed the case for hydrocarbon flames [23], which are the most common type of flames seen in nature. Other types of flames, such as blue liquefied petroleum gas flames, are not considered in this paper since they do not represent the typical flame seen in a surveillance or catastrophe scene.

For the type of flames considered (hydrocarbon flames), it is noticed that for a given fire pixel, the value of red channel is greater than the green channel, and the value of the green channel is greater than the value of blue channel, as illustrated in Fig. 1.

Several additional characteristics also hold, which are discussed in the following, where a color detection metric is proposed. This detection metric is used to generate the PFM, which will then be further analyzed with the other non-color fire features discussed in Sections III-B–III-F. Notice that this metric can also be employed in the systems discussed in Section II which use naive color thresholds to generate their PFM.

1) *Proposed Color Based Detection Metric:* Let a fire pixel at position $(m, n)$ in an image be represented by $\mathbf{f}(m, n)$, where

$$\mathbf{f}(m,n) = \begin{bmatrix} f_R(m,n) \\ f_G(m,n) \\ f_B(m,n) \end{bmatrix}$$

and $f_R$, $f_G$, and $f_B$ are the red, green, and blue channels representation of $\mathbf{f}$, respectively.

Let $\bar{f}_R$, $\bar{f}_G$, and $\bar{f}_B$ represent the sample average of the pixels in a fire image region, for the red, green, and blue channels, as shown in Fig. 1.

Interpreting $\bar{f}_R$, $\bar{f}_G$, and $\bar{f}_B$ as random variables, we employ a Gaussian model for these variables, such that $\bar{f}_R \sim \mathcal{N}(\mu_{\bar{f}_R}, \sigma^2_{\bar{f}_R})$, $\bar{f}_G \sim \mathcal{N}(\mu_{\bar{f}_G}, \sigma^2_{\bar{f}_G})$, and $\bar{f}_B \sim \mathcal{N}(\mu_{\bar{f}_B}, \sigma^2_{\bar{f}_B})$. Notice that a distinction should be made between the distribution of the pixels in $f_R$ and the distribution of $\bar{f}_R$, i.e., the distribution of the sample average of the pixels in $f_R$. The same is valid for $\bar{f}_G$ and $\bar{f}_B$.

With these assumptions, let us define

$$D_{C_R} = p_{\bar{f}_R}(\bar{f}_{R\text{obs}}) / p_{\bar{f}_R}(\mu_{\bar{f}_R}) \tag{1}$$

$$D_{C_G} = p_{\bar{f}_G}(\bar{f}_{G\text{obs}}) / p_{\bar{f}_G}(\mu_{\bar{f}_G}) \tag{2}$$

$$D_{C_B} = p_{\bar{f}_B}(\bar{f}_{B\text{obs}}) / p_{\bar{f}_B}(\mu_{\bar{f}_B}) \tag{3}$$

where $p_x(x_0)$ represents the evaluation of the probability density function (PDF) of a random variable $x$ at value $x_0$. In this case, $\bar{f}_{R\text{obs}}$ represents the average value in the red channel of an observed set of pixels. Fig. 2 illustrates that the maximum value for $D_{C_R}$ is obtained when $\bar{f}_{R\text{obs}} = \mu_{\bar{f}_R}$.

$D_{C_R}$ can be interpreted as a normalized metric that indicates the probability that a given region represents fire according to the red channel distribution. For example, if in (1) $\bar{f}_{R\text{obs}}$ is very close to $\mu_{\bar{f}_R}$, $D_{C_R}$ is very close to 1 and we assume with probability $D_{C_R}$ that the observed region represents a fire region (considering the red channel *only*). To extend this to the three color channels, in the following we employ $D_{C_R}$, $D_{C_G}$, and $D_{C_B}$ as given in (4).

Using the definitions (1)–(3), the proposed detection metric $D_C$ to indicate whether the observed region represents fire is

given as

$$D_C = D_{C_R} + D_{C_G} + D_{C_B} - (D_{C_R}D_{C_G} + D_{C_R}D_{C_B} + D_{C_G}D_{C_B}) + D_{C_R}D_{C_B}D_{C_G}. \quad (4)$$

If $\bar{f}_{R\text{obs}}$, $\bar{f}_{G\text{obs}}$, and $\bar{f}_{B\text{obs}}$ can be assumed independent, $D_C$ can be interpreted as the degree of confidence—represented by a probability—that a set of pixels represents a fire region (based only on color analysis). If we assume that $\bar{f}_{R\text{obs}}$, $\bar{f}_{G\text{obs}}$, and $\bar{f}_{B\text{obs}}$ are correlated, $D_C$ is an approximation that depends on the correlation level. In practice, however, $D_C$ yields meaningful results. This is illustrated in Section V, in which comparisons between the theoretical error rate based on $D_C$ and results from real data show good correspondence.

Equation (4) is based on fundamentals of probability theory, and its derivation is given in Appendix I.

Based on the metric $D_C$ a binary image PFM is generated for each frame, such that

$$\text{PFM}(m,n) = \begin{cases} 0, & \text{if } D_C(m,n) < \lambda_C \\ 1, & \text{otherwise} \end{cases} \quad (5)$$

where $\lambda_C$ is a confidence threshold level and the values 1 or 0 indicate the presence of absence of fire at the corresponding location in the image $\mathbf{f}$. The threshold $\lambda_C$ is the same for all pixel locations. However, in Section III-F, we propose a weighting that modifies $\lambda_C$ according to the position $(m,n)$ in the image.

2) *Color Metric Error Rate:* The variables $D_{C_R}$, $D_{C_G}$, and $D_{C_B}$ in (1)–(3) follow an exponential distribution. To determine theoretically the PDF of $D_C$, one could use the sum and difference properties for independent random variables [24]. This property states that the PDF of the sum of random variables is given by the convolution of their respective PDFs and that the PDF of difference of random variables is given by the cross-correlation of their PDFs. However, because of the correlation between some terms in (4), ($D_{C_R}$ and $D_{C_R}D_{C_G}$, for example), an analytical computation of the PDF of $D_C$ becomes very complex. In this case, we estimate this PDF via Monte Carlo simulations and nonlinear least squares curve fitting [25]. From our results, we find that $D_C$ follows an exponential distribution with the rate parameter $\lambda$.

Once we determine $\lambda$, it is possible to find the theoretical error rate of metric $D_C$. The maximum likelihood estimator for $\lambda$ is given by [26]

$$\lambda = \frac{1}{E\{D_C\}}. \quad (6)$$

In Appendix II, we show that $E\{D_C\}$ is given by

$$\mu_{D_C} = E\{D_C\} = \frac{\sqrt{2\pi}}{2\pi}\left(\frac{1}{C_R\sigma_{f_R} + C_G\sigma_{f_G} + C_B\sigma_{f_B}}\right) - \frac{1}{2\pi}\left(\frac{1}{C_RC_G\sigma_{f_R}\sigma_{f_G} + C_RC_B\sigma_{f_R}\sigma_{f_B} + C_GC_B\sigma_{f_G}\sigma_{f_B}}\right) + \left(\frac{\sqrt{2\pi}}{2\pi}\right)^3 \frac{1}{C_RC_GC_B\sigma_{f_R}\sigma_{f_G}\sigma_{f_B}} \quad (7)$$

where $C_R = p_{\bar{f}_R}(\mu_{\bar{f}_R})$, $C_G = p_{\bar{f}_G}(\mu_{\bar{f}_G})$, and $C_B = p_{\bar{f}_B}(\mu_{\bar{f}_B})$.

(a) (b)

Fig. 3. Illustration of the change in fire pixel area from frame to frame. (a) Fire area = 1692 pixels. (b) Fire area = 2473 pixels.

Based on the error rate for the exponential distribution [27], the detection error rate using $D_C$ is given by

$$R(\lambda_C) = e^{-\frac{\lambda_C}{\lambda}} \quad (8)$$

which indicates the percentage of fire pixels classified as non-fire. The experiments in Section V illustrate the applicability of this error rate.

Considering (13), we refer to the concatenation of pixels "1" as fire blobs in this paper. The PFM is then processed with a connected components algorithm so that the potential fire blobs are concatenated in a contiguous region.

Notice that the threshold $\lambda_C$ should be very permissive and many non-fire regions may be included in the PFM. For this reason, additional analysis is necessary to further refine the results. To define a real burning fire, in addition to using chromatics, statistical and dynamic features are usually adopted to distinguish other fire aliases [10], [12]. Examples of these fire dynamics include the change in shape, flame movement and flickering. The statistical and dynamic fire features proposed in this paper are discussed next.

### B. Randomness of Area Size

For the estimated fire pixel area, because of the fire flickering, a change in the area size of the PFM occurs from frame to frame, as illustrated in Fig. 3. Non-fire areas have a less random change in the area size. The normalized area change $\Delta A_i$ for the $i$th frame is given by

$$\Delta A_i = \frac{|A_i - A_{i-1}|}{A_i} \quad (9)$$

where $A_i$ corresponds to the area of the fire blobs representing the potential fire regions in the PFM. In case a hard decision rule is used, fire is assumed if $\Delta A_i > \lambda_A$, where $\lambda_A$ is a decision threshold.

### C. Boundary Roughness

As discussed in Section II, in [10], for example, the authors represent the shape of fire regions using Fourier descriptors (FD) [28], based on the coefficients of the Fourier transform. However, in a retrieval application, this solution presents two drawbacks: 1) retrieval demands a very high processing speed, and the evaluation of the FD for every frame is a very time consuming operation, specially in high resolution images; and 2) although the FD are excellent shape descriptors, for fire detection purposes the real feature of interest is the

Fig. 4. Illustration of the convex hull (red line) used to evaluate the boundary roughness of the blob.

randomness or roughness of the shape, and not the shape itself, as fire does not have a specific boundary characteristics. Therefore, we propose the use the boundary roughness of the potential fire region as a feature, given by the ratio between perimeter and convex hull perimeter [29]. The convex hull of a set of pixels $S$ is the smallest convex set containing $S$, as illustrated by the red curve in Fig. 4. The boundary roughness is given by

$$B_R = P_S / P_{CH_S}$$

where $P_S$ is the perimeter of $S$ and $P_{CH_S}$ is the perimeter of the convex hull of $S$. To compute the perimeter, a simple approach is to count the number of pixels connected horizontally and vertically plus $\sqrt{2}$ times the number of pixels connected diagonally, as described in [29]. Similarly to (9), if a hard decision rule is used, fire is assumed if $B_R > \lambda_{B_R}$, where $\lambda_{B_R}$ is a decision threshold.

Experiments illustrate that this is an excellent and computationally efficient discriminant for the shape of fire regions, yielding similar results to the use of FD, however with much lower computational complexity.

### D. Surface Coarseness

Unlike other false-alarm regions, like a yellow traffic sign, for example (Fig. 5), fire regions have a significant amount of variability in the pixel values. Filter banks are frequently used in texture analysis when trying to describe a given pattern [28]. In the case of fire, however, it is very hard to describe its texture with any given model. The randomness observed in fire can vary significantly in frequency response (periodicity is often not present) and gradient angles, for example. The variance is a well-known metric [28], [29] to indicate the amount of coarseness in the pixel values.

Hence, we use the variance of the blobs as a feature to help eliminating non-fire blobs in the PFM. Therefore, fire is assumed if the blob has a variance $\sigma > \lambda_\sigma$, where $\lambda_\sigma$ is determined from a set of experimental analyses. Fig. 5 illustrates how the use of the variance can reduce the false-alarm rate of the PFM, for an illustrative threshold $\lambda_\sigma = 50$.

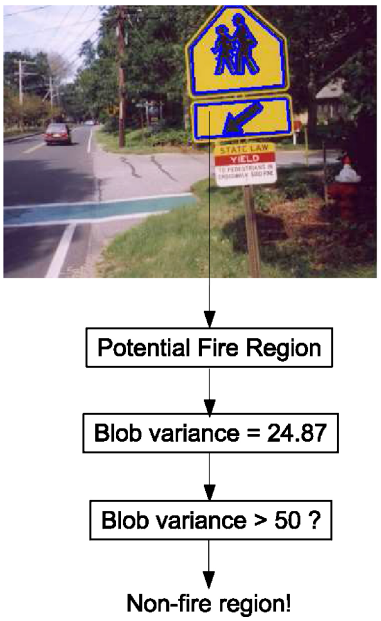


Fig. 5. Example of eliminating potential fire regions through variance analysis *only*.

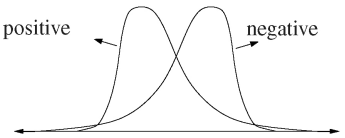


Fig. 6. Illustration of the effect of positive and negative skewness on a distribution.

### E. Skewness

The skewness measures the degree of asymmetry of a distribution around its mean [24]. It is zero when the distribution is symmetric, positive if the distribution shape is more spread to the right and negative if it is more spread to the left, as illustrated in Fig. 6.

As discussed in Section III-A, fire regions have high pixel values for the green and specially for the red channel. Very often, we observe a saturation in the red channel, leading the histogram to the upper side of the range, as illustrated in Fig. 7. This causes the skewness of this distribution to have a high negative value. For this reason, we employ the skewness as an useful feature to identify fire regions. Let the sample skewness $\gamma_R$ of the red channel be defined as

$$\gamma_R = \frac{\frac{1}{J^2}\sum_{m=1}^{J}\sum_{n=1}^{J}[f_R(m,n) - \bar{f}_R]^3}{\sigma_{f_R}^3} \tag{10}$$

where $J$ is the number of pixels in the blob. A potential fire region present at frame $i$ is assumed as real fire if

$$\gamma_{R_i} < \lambda_{\gamma_R} \tag{11}$$

where $\lambda_{\gamma_R}$ is a decision threshold. Experiments illustrate that fire regions usually have $\gamma_R < -1$, and this is the value we use in the experiments in Section V.

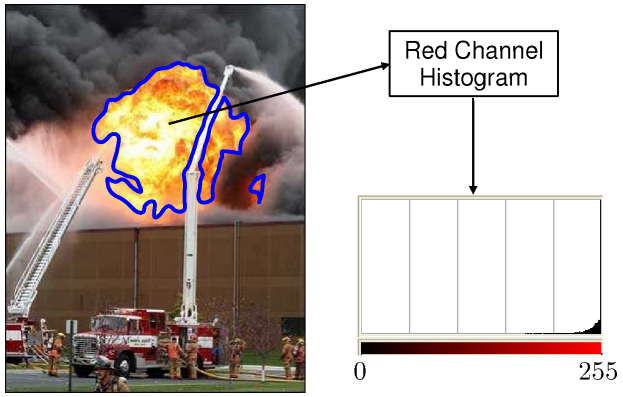


Fig. 7. Illustration of the saturation effect in the histogram of the red channel of the fire regions inside the blue boundaries.

Fig. 8. Illustration of images containing fire.

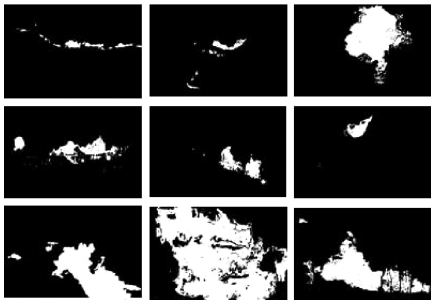

Fig. 9. Illustration of fire segmentation.

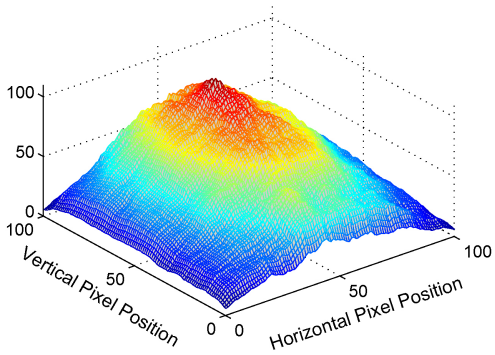


Fig. 10. 3-D representation of $s$.

### F. Spatial Distribution of Fire

One important characteristic of "human recorded" videos (i.e., not surveillance cameras) is that the fire is the most important semantic part of the image for the camera-man/woman. For this reason, fire is usually located in the central area of the frame.

From a set of 120 images color images $\mathbf{a}_i$, $i = 1 \ldots 120$ containing fire, we manually segmented the fire regions (generating the ground truth), setting the "fire pixels" to 1 and the "non-fire pixels" to zero. A few examples of test images are given in Fig. 8, and their corresponding segmented versions are illustrated in Fig. 9. We refer to the segmented binary images as $a_{s_i}$. Let $s$ be a new image given by the sum of all the segmented images, such that $s = \sum_{i=1}^{120} a_{s_i}$. A 3-D representation of $s$ is given in Fig. 10. Projecting the pixels in $s$ to the vertical axis, we obtain the distributions presented in Figs. 11 and 12, as a function of vertical and horizontal positions, respectively.

In Fig. 11, we observe the relationship between the vertical position and the probability of occurrence of fire in a given part of an image containing fire.

Using a histogram-based PDF estimation [25], the distribution in Fig. 11 is well represented by a non-central chi-square distribution [24] with two degrees of freedom and non-centrality equal to 4.5. This is intuitively coherent as fire has a well-defined lower burning base which extends to the top of the image. Similarly, on the horizontal axis the probability of occurrence of fire is approximated by a generalized normal distribution, with standard deviation equal to 3.10, gamma parameter equal to 1.82, and mean on the center of the horizontal axis, as illustrated in Fig. 12.

We use this information to weight the confidence from the result of the color analysis given in (5), depending on the location where potential fire is found. We define this weighting as $w(m, n)$ such that

$$w(m,n) = \frac{1}{2}\left(\frac{g_h(m)}{max_{g_h}} + \frac{g_v(n)}{max_{g_v}}\right) \tag{12}$$

where $m$ and $n$ are the pixel coordinates and $g_h(m)$ and $g_v(m)$ are the functions describing the vertical and horizontal spatial distributions of the fire, respectively (shown in Figs. 11 and 12). The variables $\max_{g_h}$ and $\max_{g_v}$ represent the maximum values that the functions may take, acting as a normalizing factor. In Fig. 11, for example, $\max_{g_v} = 0.1$.

In this case, (5) becomes

$$\text{PFM}(m,n) = \begin{cases} 0, & \text{if } D_C(m,n) < w(m,n)\lambda_C \\ 1, & \text{otherwise.} \end{cases} \tag{13}$$

## IV. Classification

Considering a stochastic interpretation of the features discussed in Section III, the Bayes classifier [28] is employed to combine the features, although it is clear that different statistical classifiers could also be tested.

For each frame $i$, naive set of PFMs is initially created based on the set of rules for color, from Section III-A. For each PFM,

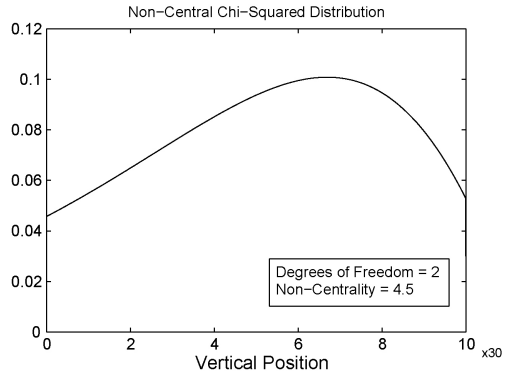


Fig. 11. Plot of a chi-square probability density function, representing the distribution of the pixel count on the vertical axis as a function of the position, where 0 represents the bottom of the image.

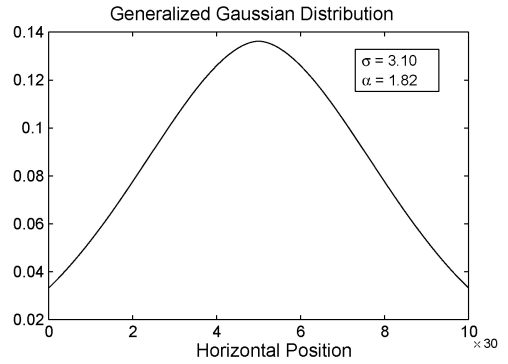


Fig. 12. Plot of a generalized Gaussian probability density function, representing the distribution of the pixel count on the horizontal axis as function of the position, where 0 represents the left of the image.

a vector $\boldsymbol{d}$ of features is obtained as

$$\boldsymbol{d} = \begin{bmatrix} \Delta A \\ B_R \\ \sigma \\ \gamma_R \end{bmatrix}. \tag{14}$$

The features used are the ones discussed in the previous section: area size change, boundary roughness, variance, and red channel skewness. The features are combined according to the Bayes classifier.

In order to classify the class fire from the class non-fire, the Bayes classifier needs to estimate the mean and the variance of each class. Therefore, it requires a statistical "training," based on observed values, to determine a decision function that separates the classes. Let $b$ indicate a flag that represents one of the two possible classes: $b = 1$ represents the fire class and $b = 0$ represents the non-fire class. Using this notation, the Gaussian density of the vector in the *fire* class has the form

$$p(\boldsymbol{d}/b = 1) = \frac{1}{2\pi|\boldsymbol{C_1}|} e^{-\frac{1}{2}(\boldsymbol{d}-\boldsymbol{m_1})^T \boldsymbol{C_1}^{-1}(\boldsymbol{d}-\boldsymbol{m_1})} \tag{15}$$

where $\boldsymbol{m_1} = E\{\boldsymbol{d}\}$ is the mean vector in the fire class and $\boldsymbol{C_1} = E\{(\boldsymbol{d}-\boldsymbol{m_1})(\boldsymbol{d}-\boldsymbol{m_1})^T\}$ is the covariance matrix in the fire class. Similar formulation is obtained for the non-fire class, yielding

$$p(\boldsymbol{d}/b = 0) = \frac{1}{2\pi|\boldsymbol{C_0}|} e^{-\frac{1}{2}(\boldsymbol{d}-\boldsymbol{m_0})^T \boldsymbol{C_0}^{-1}(\boldsymbol{d}-\boldsymbol{m_0})}. \tag{16}$$

Under the above assumptions, the Bayes classifier decision function in the fire class is described by

$$f_1(\boldsymbol{d}) = \ln\Pr(b = 1) - \frac{\ln|\boldsymbol{C_1}|}{2} - \frac{(\boldsymbol{d}-\boldsymbol{m_1})^T \boldsymbol{C_1}^{-1}(\boldsymbol{d}-\boldsymbol{m_1})}{2} \tag{17}$$

where ln represents the natural logarithm operation. Correspondingly, for the non-fire class, the decision function is

$$f_0(\boldsymbol{d}) = \ln\Pr(b = 0) - \frac{\ln|\boldsymbol{C_0}|}{2} - \frac{(d-m_0)^T C_0^{-1}(d-m_0)}{2}. \tag{18}$$

Finally, the decision surface separating the two classes is

$$f_{10} = f_1(\boldsymbol{d}) - f_0(\boldsymbol{d}) = 0. \tag{19}$$

Fig. 16 illustrates a 3-D decision function separating fire from non-fire. A more detailed description on how to combine the features using this technique can be found in [26] and [29]. A block diagram of the process is given in Fig. 13. Using this classification framework, the naive thresholds $\lambda_A$, $\lambda_{B_R}$, $\lambda_{\gamma_R}$, and $\lambda_\sigma$ discussed in Section III are not applied, but only give the reader a practical reference for the typical values for these parameters.

Although some features have better classification power than others, because all the discussed features are useful to discriminate fire from non-fire, combining them increases the distance between these two classes, and consequently reduces the detection error rate [28], at the expense of increasing computational complexity.

## V. Experiments

In the experiments, we used a selection of test videos from the MESH [3] database of news content. This database is formed of several instances of catastrophe related videos from the Deutsche Welle broadcaster. It contains several news reports related to fire events. They include different kinds of fires such as building, wildland and residential fire, containing shots captured at day time, dusk or night time. This diversity is convenient to evaluate the performance of the system under different lighting and quality conditions. The video selection also contains many shots of objects with fire-like appearances such as sunsets and artificial background from the news program, as illustrated in Fig. 15. Notice that, for this figure, a naive classification based only on the set of rules described in Section III-A would cause a wrong detection. The video resolution is $768 \times 576$ and the frame rate is 25 frames/s. There are approximately 532 min of video (or 798 000 frames).

In addition to the MESH database, we have tested videos from surveillance cameras available online and also from the database in http://signal.ee.bilkent.edu.tr/VisiFire.

### A. Experiment 1

This experiment illustrates the applicability of the metric $D_C$. Moreover, it shows an excellent correspondence between

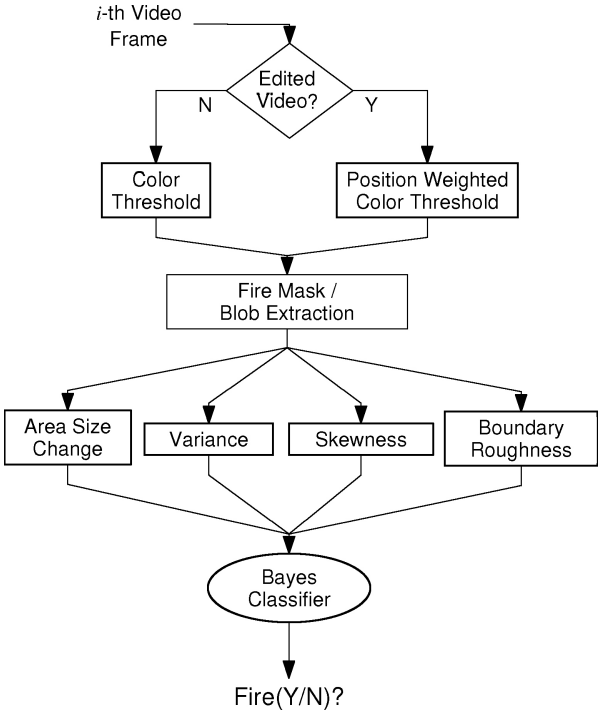


Fig. 13. Block diagram illustrating the fire detection process for each frame $i$, including the PFM generation, the extraction of features and the classification according to the Bayes classifier. When edited newscast videos are considered, the decision block "Edited Video?" indicates how the algorithm should compute the PFM: "Color Threshold"—corresponding to (13) or "Position Weighted Color Threshold"—corresponding to (13).

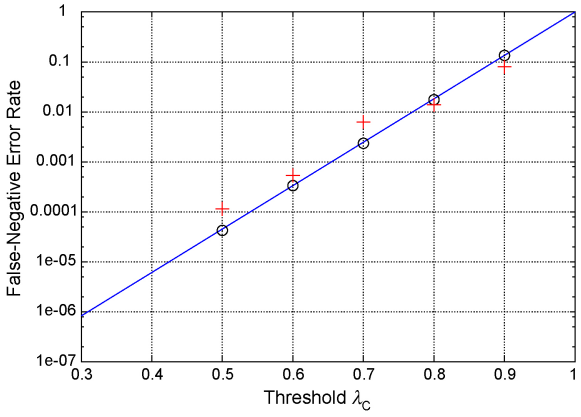


Fig. 14. Plot of the theoretical false-negative error rate based only the color metric $D_C$. The black circles represent the experimental error rates from synthetic simulations. The red crosses represent the practical error rates using the real video database.


Fig. 15. Illustration of an artificial fire-like region, with potential false-negative.

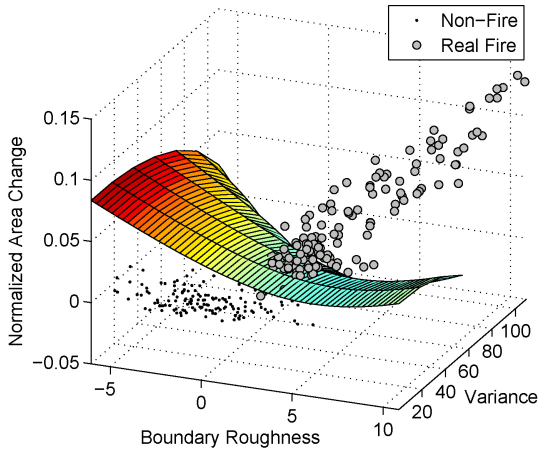


Fig. 16. Illustration of a surface separating frames from fire to non-fire classes, based on the features roughness, variance and normalized area change.

the error rate analysis provided in Section III-A2 and error rates from synthetic simulations. In Fig. 14, we plot the theoretical false-negative error rate, given in (8). In this figure, the circle marks represent the experimental error rates from synthetic simulations, where no real video is analyzed. Instead, these error rates were determined from random signals with the same statistical characteristics assumed for the fire regions (as discussed in Section III-A), which were computer generated.

The red crosses represent the results using samples from the real tested videos. In this case, we can see a discrepancy between the theoretical error rate and the error rate from real experimental results. This difference is expected due to a relaxation in the statistical assumptions employed in the error analysis. Despite the difference, the analysis still yield a reasonable correspondence between theory and practice, such that the user can estimate of the system performance according to (8). Notice that the error rate increases as the threshold approaches 1.

### B. Experiment 2

The frames are classified as "contains fire" or "does not contain fire," as discussed in Section IV. For training the classifier, 75 instances of fire in video sequences were used, generating a 4-D decision surface. Fig. 16 illustrates a 3-D separating surface for discriminating fire from non-fire regions, based on the features boundary roughness, variance, and normalized area change.

The results using the proposed features are presented in Table I. This table shows the false positive (wrongly assume the presence of fire) rate and the false negative (wrongly assume the absence of fire) rate. The rows corresponding to each feature represent the error rates when that feature only is used to classify fire from non-fire, after the color-based fire segmentation is done. The table also indicates how the different features increase the performance of the system and compare to each other. The row "Combination" corresponds to the results when all the features are combined, as illustrated in Fig. 13.

TABLE I
EXPERIMENTAL ERROR RATES: PERFORMANCE COMPARISON AMONG USED FEATURES

| Features Used | False-Positive | False-Negative |
|---|---|---|
| Color | 9.37% | 0.033% |
| + Position (edited videos) | 6.12% | 0.028% |
| + Skewness | 1.95% | – |
| + Roughness | 3.70% | – |
| + Area change | 2.26% | – |
| + Variance | 7.11% | – |
| Combination | 0.68% | – |

TABLE II
ERROR RATE COMPARISON WITH DIFFERENT METHODS

| Method | False-Positive | False-Negative |
|---|---|---|
| Proposed | 0.68% | 0.028% |
| [8] | 0.9% | 0.04% |
| [10] | 0.0% | 0.1% |
| [11] | 9.9% | 1.0% |
| [20] | 0.297% | 12.36% |
| [19] | 0.1% | 0% |

Comparisons with other methods in the literature are presented in Table II. This table indicates the reference being compared (left column) and its reported error rate. The results described in [10] and [19], for example, yield very low error rates. However, [19] assumes the camera is stationary and [10] makes use of frequency transforms and motion tracking, requiring more computational processing time, making them unsuitable for video retrieval. In [11], a good false-negative rate is achieved, however with a high false-positive (9.9%), which is considerably higher than the rate in the proposed method. The results reported in [20], on the other hand, indicate a very low false-positive rate at the expense of a high number of false-negatives. The second row in the table [8] shows results of an earlier version of the proposed system, which had an inferior performance mainly due to the naive color thresholding.

## VI. CONCLUSION

In this paper, we have proposed a new detection metric based on color for fire detection in videos. In addition, we have exploited important visual features of fire, like boundary roughness and skewness of the fire pixel distribution. The skewness, in particular, is a very useful descriptor because of the frequent occurrence of saturation in the red channel of fire regions. Also, we have proposed modifications to motion-based features. For newscast videos, we model the probability of occurrence of fire as a function of the position, yielding an efficient performance.

In contrast to other methods which extract complicated features, the features discussed here allow very fast processing, making the system applicable not only for real time fire detection, but also for video retrieval in news contents, which require faster than real-time analysis. The experiments illustrate the applicability of the method, with an average false-positive rate of 0.68% and a false-negative rate of 0.028%. Although out of the scope of this paper, in a real retrieval system such as MESH [3], information from automatic speech recognition [30] can also be used to improve the system reliability. Further work includes using a Markovian approach to formalize the feature dependence between adjacent frames and how the features evolve in time.

## APPENDIX I

This appendix shows how (4) can be interpreted as a degree of confidence (probability) using the metrics given in (1)–(3).

In probability, the inclusion-exclusion principle [31] states that for random events $A_i$

$$P\left(\bigcup_{i=1}^{n} A_i\right) = \sum_{k=1}^{n}(-1)^{k-1} \sum_{\substack{I\subset\{1,\ldots,n\}\\ |I|=k}} P(A_I) \tag{20}$$

where the second sum on the right-hand side of the equation is performed over all subsets $I$ of the indices $1, \ldots, n$, which contain exactly $k$ elements, and

$$A_I = \bigcap_{i\in I} A_i \tag{21}$$

represents the intersection of all those $A_i$ with index in $I$.

For $n = 2$, (20) represents the well-known addition law of probabilities based on the Kolmogorov probability axioms [32], given by

$$P(A \cup B) = P(A) + P(B) - P(A \cap B) \tag{22}$$

for events $A$ and $B$. For $n = 3$, we have

$$\begin{aligned} P(A \cup B \cup C) = {} & P(A) + P(B) + P(C) - P(A \cap B) \\ & - P(A \cap C) - P(B \cap C) + P(A \cap B \cap C). \end{aligned} \tag{23}$$

Considering that $D_{C_R}$ in (1) represents a probability, we can replace $P(A)$ with $D_{C_R}$. The same is valid for $D_{C_G}$ and $D_{C_B}$. Therefore, if we let $P(A \cup B \cup C) = D_C$, we may write

$$\begin{aligned} D_C = {} & D_{C_R} + D_{C_G} + D_{C_B} - (D_{C_R}D_{C_G} + D_{C_R}D_{C_B} \\ & + D_{C_G}D_{C_B}) + D_{C_R}D_{C_B}D_{C_G}. \end{aligned} \tag{24}$$

This is the result shown in (4) and it is interpreted as the degree of confidence (represented by a probability) that a set of pixels represents a fire region.

## APPENDIX II

This appendix derives the result presented in (7). The expected value of $D_C$ is given by

$$\begin{aligned} \mu_{D_C} = E\{D_C\} = E\{ & D_{C_R} + D_{C_G} + D_{C_B} \\ & - (D_{C_R}D_{C_G} + D_{C_R}D_{C_B} + D_{C_G}D_{C_B}) \\ & + D_{C_R}D_{C_B}D_{C_G}\}. \end{aligned} \tag{25}$$

Using the linearity property of expected values, each term separated by addition or subtractions in (25) can be analyzed separately. The first term is given by

$$\begin{aligned} E\{D_{C_R}\} &= E\{p_{\bar{f}_R}(\bar{f}_{R\text{obs}})/p_{\bar{f}_R}(\mu_{\bar{f}_R})\} \\ &= E\{p_{\bar{f}_R}(\bar{f}_{R\text{obs}})\}/C_R \end{aligned} \tag{26}$$

where $C_R = p_{\bar{f}_R}(\mu_{\bar{f}_R})$ is a constant. Recall from Section III-A that $\bar{f}_{R\text{obs}} \sim \mathcal{N}(\mu_{\bar{f}_R}, \sigma^2_{\bar{f}_R})$ and $p_x(x_0)$ represents the evaluation of the PDF of a random variable $x$ at value $x_0$. The change of variables theorem for expected values [33] states that, for a function $g(x)$, where $x$ is a random variable

$$E\{g(x)\} = \int_{-\infty}^{\infty} g(x) f(x) dx \tag{27}$$

where $f(x)$ is the PDF of x. Using (27) to solve (26) yields

$$\begin{aligned} E\{D_{C_R}\} &= \frac{1}{C_R} \int_{-\infty}^{\infty} \left( \frac{1}{\sigma_{f_R}\sqrt{2\pi}} e^{\frac{\left(\bar{f}_{R\text{obs}} - \mu_{\bar{f}_R}\right)^2}{2\sigma^2_{\bar{f}_R}}} \right. \\ &\quad \left. \frac{1}{\sigma_{f_R}\sqrt{2\pi}} e^{-\frac{\left(\bar{f}_{R\text{obs}} - \mu_{\bar{f}_R}\right)^2}{2\sigma^2_{\bar{f}_R}}} \right) d\bar{f}_{R\text{obs}} \\ &= \frac{1}{C_R 2\pi\sigma^2_{\bar{f}_R}} \int_{-\infty}^{\infty} e^{-\frac{\left(\bar{f}_{R\text{obs}} - \mu_{\bar{f}_R}\right)^2}{\sigma^2_{\bar{f}_R}}} d\bar{f}_{R\text{obs}} \\ &= \frac{1}{C_R 2\pi\sigma^2_{\bar{f}_R}} \sigma_{f_R}\sqrt{2\pi} = \mu_{D_{C_R}}. \end{aligned} \tag{28}$$

A similar analysis is valid for the terms $D_{C_G}$ and $D_{C_B}$ in (25).

For the joint term $D_{C_R} D_{C_G}$, assuming that $D_{C_R}$ and $D_{C_G}$ are independent, it follows that

$$\begin{aligned} \mu_{D_{C_R} D_{C_G}} &= E\{D_{C_R} D_{C_G}\} \\ &= \mu_{D_{C_R}} \mu_{D_{C_G}} = \frac{1}{2\pi C_R C_G \sigma_{f_R} \sigma_{f_G}}. \end{aligned} \tag{29}$$

For the joint term $D_{C_R} D_{C_G} D_{C_B}$, assuming that $D_{C_R}$, $D_{C_G}$, and $D_{C_B}$ are independent, an analysis similar to (29) yields

$$\mu_{D_{C_R} D_{C_G} D_{C_B}} = E\{D_{C_R} D_{C_G} D_{C_B}\} = \mu_{D_{C_R}} \mu_{D_{C_G}} \mu_{D_{C_G}}. \tag{30}$$

Replacing the results from (28) to (30) into (25) yields

$$\begin{aligned} \mu_{D_C} = E\{D_C\} &= \frac{\sqrt{2\pi}}{2\pi} \left( \frac{1}{C_R\sigma_{f_R} + C_G\sigma_{f_G} + C_B\sigma_{f_B}} \right) \\ -\frac{1}{2\pi} &\left( \frac{1}{C_R C_G \sigma_{f_R}\sigma_{f_G} + C_R C_B \sigma_{f_R}\sigma_{f_B} + C_G C_B \sigma_{f_G}\sigma_{f_B}} \right) \\ &+ \left( \frac{\sqrt{2\pi}}{2\pi} \right)^3 \frac{1}{C_R C_G C_B \sigma_{f_R}\sigma_{f_G}\sigma_{f_B}} \end{aligned} \tag{31}$$

which is the result presented in (7).

## ACKNOWLEDGMENT

The authors would like to thank the anonymous reviewers for their valuable comments and suggestion.

## REFERENCES

[1] X. Wu, C. Ngo, and Q. Li, "Threading and autodocumenting news videos: A promising solution to rapidly browse news topics," *IEEE Signal Process. Mag.*, vol. 3, no. 2, pp. 59–68, Mar. 2006.

[2] Y. Wang, Z. Liu, and J. C. Huang, "Multimedia content analysis-using both audio and visual clues," *IEEE Signal Process. Mag.*, vol. 17, no. 6, pp. 12–36, Nov. 2000.

[3] MESH, *Multimedia Semantic Syndication for Enhanced News Service*, European Commission Project, IST 6th Framework Programme. Available: http://www.mesh-ip.eu/

[4] KSPACE, *Knowledge Space of Semantic Inference for Automatic Annotation and Retrieval of Multimedia Content*, European Commission Project, IST 6th Framework Programme. Available: http://k-space.eu/

[5] C. L. Lai, J. C. Yang, and Y. H. Chen, "A real time video processing based surveillance system for early fire and flood detection," in *Proc. IEEE Instrum. Meas. Technol. Conf.*, Warsaw, Poland, May 2007, pp. 1–6.

[6] P. Huang, J. Su, Z. Lu, and J. Pan, "A fire-alarming method based on video processing," in *Proc. IEEE Int. Conf. Intell. Inform. Hiding Multimedia Signal Process.*, Dec. 2006, pp. 359–364.

[7] T. Celik, H. Demirel, H. Ozkaramanli, and M. Uyguroglu, "Fire detection in video sequences using statistical color model," in *Proc. IEEE Int. Conf. Acoust. Speech Signal Process.*, vol. 2. Toulouse, France, May 2006, p. II.

[8] P. V. K. Borges, J. Mayer, and E. Izquierdo, "Efficient visual fire detection applied for video retrieval," in *Proc. 16th Eur. Signal Process. Conf.*, Aug. 2008.

[9] B. U. Toreyin and A. E. Cetin, "Online detection of fire in video," in *Proc. IEEE Conf. Comput. Vision Pattern Recognit.*, Jun. 2007, pp. 1–5.

[10] C. Liu and N. Ahuja, "Vision-based fire detection," in *Proc. Int. Conf. Pattern Recognit.*, vol. 4. Aug. 2004, pp. 134–137.

[11] T. Celik, H. Ozkaramanli, and H. Demirel, "Fire pixel classification using fuzzy logic and statistical color model," in *Proc. Int. Conf. Acoust. Speech Signal Process.*, vol. 1. Apr. 2007, pp. 1205–1208.

[12] T. Chen, P. Wu, and Y. Chio, "An early fire-detection method based on image processing," in *Proc. IEEE Int. Conf. Image Process.*, vol. 3. Oct. 2004, pp. 1707–1710.

[13] S. C. Liew, A. Lim, and L. K. Kwoh, "A stochastic model for active fire detection using the thermal bands of modis data," *IEEE Geosci. Remote Sensing Lett.*, vol. 2, no. 3, pp. 337–341, Jul. 2005.

[14] Y. Li, A. Vodacek, R. L. Kremens, A. Ononye, and C. Tang, "A hybrid contextual approach to wildland fire detection using multispectral imagery," *IEEE Trans. Geosci. Remote Sensing*, vol. 43, no. 9, pp. 2115–2126, Sep. 2005.

[15] A. Abuelgasim and R. Fraser, "Day and night-time active fire detection over North America using NOAA-16 AVHRR data," in *Proc. IEEE Int. Geosci. Remote Sensing Symp.*, vol. 3. Jun. 2002, pp. 1489–1491.

[16] G. Healey, D. Slater, T. Lin, B. Drda, and A. D. Goedeke, "A system for real-time fire detection," in *Proc. IEEE Conf. Comput. Vision Pattern Recognit.*, Jun. 1993, pp. 605–606.

[17] W. Phillips, III, M. Shah, and N. da Vitoria Lobo, "Flame recognition in video," in *Proc. IEEE Workshop Applicat. Comput. Vision*, Dec. 2000, pp. 224–229.

[18] T. Celik and H. Demirel, "Fire detection in video sequences using a generic color model," *Fire Safety J.*, vol. 44, no. 2, pp. 147–158, Feb. 2009.

[19] B. U. Toreyin, Y. Dedeoglu, U. Gudukbay, and E. Cetin, "Computer vision-based method for real-time fire and flame detection," *Pattern Recognit. Lett.*, vol. 27, no. 4, pp. 49–58, 2006.

[20] C. Ho, "Machine vision-based real-time early flame and smoke detection," *Meas. Sci. Technol.*, vol. 20, no. 4, 045502 (13 pp), Apr. 2009.

[21] Z. Xiong, R. E. Caballero, H. Wang, A. M. Finn, and P. Peng, "Video fire detection: Techniques and applications in the fire industry," in *Multimedia Content Analysis*. Berlin, Germany: Springer, 2009, pp. 339–351.

[22] B. C. Ko, K. Cheong, and J. Nam, "Fire detection based on vision sensor and support vector machines," *Fire Safety J.*, vol. 44, no. 3, pp. 322–329, Apr. 2009.

[23] C. E. Baukal, Jr., *The John Zink Combustion Handbook*, 1st ed. Boca Raton, FL: CRC Press, 2001.

[24] D. G. Manolakis, V. K. Ingle, and S. M. Kogon, *Statistical and Adaptive Signal Processing*. New York: McGraw-Hill, 2000.

[25] B. W. Silverman, *Density Estimation for Statistics and Data Analysis*, 1st ed. London, U.K.: Chapman and Hall, 1986.

[26] S. M. Kay, *Fundamentals of Statistical Signal Processing: Estimation Theory*, vol. 1. Englewood Cliffs, NJ: Prentice-Hall, 1993.

[27] S. M. Kay, *Fundamentals of Statistical Signal Processing: Detection Theory*, vol. 2, 4th ed. Englewood Cliffs, NJ: Prentice-Hall, 1998.

[28] S. Theodoridis and K. Koutroumbas, *Pattern Recognition*. New York: Academic, 2006.

[29] R. C. Gonzalez and R. E. Woods, *Digital Image Processing*. Reading, MA: Addison-Wesley, 1992.

[30] J. Junqua and J. Haton, *Robustness in Automatic Speech Recognition: Fundamentals and Applications*. Boston, MA: Kluwer, 1995.

[31] W. Szpankowski, *Average Case Analysis of Algorithms on Sequences*, 1st ed. New York: Wiley-Interscience, 2001.
[32] P. Roeper and H. Leblanc, *Probability Theory and Probability Logic*, 1st ed. Toronto, Canada: University of Toronto Press, 1999.
[33] A. Papoulis and S. U. Pillai, *Probability, Random Variables and Stochastic Processes*, 4th ed. New York: McGraw-Hill, 2001.

**Paulo Vinicius Koerich Borges** (M'03) received the B.E. and M.S. degrees in electrical engineering from the Federal University of Santa Catarina (UFSC), Florianópolis, Brazil, in 2002 and 2004, respectively, and the Ph.D. degree on the subject of digital watermarking and data hiding from Queen Mary, University of London (QMUL), London, U.K., and UFSC, in 2007.

In 2001, he was a Visiting Research Student in the subject of image restoration with the University of Manchester, Manchester, U.K. From 2007 to 2008, he was a Post-Doctoral Researcher with QMUL, where he worked on the European Union Information Society Technologies MESH Project on the subject of video event detection. Since 2009, he has been a Research Scientist with the Autonomous System Laboratory, Information and Communication Technologies Center, CSIRO, Pullenvale, QLD, Australia. His current research topic is visual-based robot tracking and localization. His current research interests include video event detection/classification, video tracking, and digital watermarking, besides general image processing and pattern recognition.

Dr. Borges was a Reviewer for several international conferences and journals, and was in the Organizing Committee of the IEEE Conference on Information Visualization, the IEEE International Conference on Image Processing, and the International Workshop on Content-Based Multimedia Indexing.

**Ebroul Izquierdo** (M'95–SM'03) received the B.Sc and M.Sc degrees in applied maths from Humboldt University, Berlin, Germany, in 1987 and 1989, respectively. He received the Dr. Rerum Naturalium (Dr.rer.nat) degree for his thesis on the numerical approximation of algebraic-differential equations in 1993 from the same institution.

From 1990 to 1992, he was a Teaching Assistant with the Department of Applied Mathematics, Technical University Berlin, Berlin, Germany. From 1993 to 1997, he was an Associate Researcher with Heinrich-Hertz Institute for Communication Technology, Berlin, Germany. From 1998 to 1999, he was a Senior Research Officer with the Department of Electronic Systems Engineering, University of Essex, Essex, U.K. Since 2000, he has been with the Department of Electronic Engineering, Queen Mary, University of London, London, U.K., where he is currently the Chair of Multimedia and Computer Vision and the Head of the Multimedia and Vision Research Group with the Department of Electronic Engineering and Computer Science. He has been involved and coordinating several large European research projects over the last 12 years. He has published over 300 technical papers, including different chapters in books. His current research interests include video coding, video analysis, and visual information retrieval.

Dr. Izquierdo is an Associate Editor of several journals in the field of multimedia signal processing, including the IEEE TRANSACTIONS ON CIRCUITS AND SYSTEMS FOR VIDEO TECHNOLOGY (TCSVT) and the *EURASIP Journal on Image and Video Processing*. He has served as a Guest Editor of three special issues of the IEEE TCSVT, three special issues of the *Journal Signal Processing: Image Communication*, two special issues of the *EURASIP Journal on Applied Signal Processing and Image and Video Processing*, and several special issues in other journals in the same field. He is a Chartered Engineer, a Fellow Member of the Institution of Engineering and Technology, and a Member of the British Machine Vision Association. He has chaired and co-organized several conferences and workshops in multimedia communications, visual information retrieval, and coding technology.